

Dual-Band Low Profile SIW Cavity-Backed Antenna by Using Bilateral Slots

Bollavathi Lokeshwar^{1, *}, Dorai Venkatasekhar², and Alapati Sudhakar³

Abstract—In this paper, a design of a low profile cavity backed antenna consisting of bilateral slots is developed for generating two frequencies. Here, the whole antenna including substrate integrated waveguide (SIW) cavity is constructed from only one substrate with the height of $0.026\lambda_0$. The long transversal slot at the ground plane is excited by TE_{210} mode of the cavity and produces one hybrid mode resonance at 9.85 GHz. When the short transversal slot cut is incorporated in the top portion of the cavity, TE_{310} mode is perturbed, which results in generating an additional hybrid mode resonance at 14 GHz. Both these hybrid modes help to create a dual-band response. A sample of the proposed design is fabricated, and it has been verified experimentally that the bandwidths of the proposed design are 530 MHz (5.48%) and 440 MHz (3.15%) at lower and higher resonant frequencies, respectively. The antenna renders measured peak gains of 6.62 dBi and 6.44 dBi at 9.85 GHz and 14 GHz, respectively. The cross-polarization level of maximum -20 dB and same polarization planes are obtained at both the operating frequencies.

1. INTRODUCTION

Dual-band antennas with planar structure have attracted much attention to develop various applications for millimeter and microwave systems. To date, numerous antenna designs have been published by researchers in the literature to get a dual-frequency response. One of the most popular candidates is microstrip-line slot antenna due to its amicable characteristics such as cost savings, miniaturization, easy integration with the other planar components, and conformability to both planar and cylindrical surfaces [1–3]. To achieve unidirectional radiation pattern with high gain, typically a non-planar metallic cavity is placed behind the slot [4]. However, conventional cavity backed slot antennas (CBSA) are difficult to integrate with the arbitrarily curved surfaces, and the fabrication process would complicate the antenna structure.

Recently, many researchers are focusing inquisitively on the state-of-the-art SIW technology to design traditional metallic cavity structures in the planar substrate that implement and integrate microwave and millimeter wave components. In addition, it reduces the cost of fabrication, convenient fabrication using a printed circuit board (PCB) technology [5, 6]. The first slot antenna which encompasses both SIW cavity and feeding circuit is reported in [7]. Several designs of substrate integrated waveguide (SIW) CBSAs have been widely presented at a single band response in the literature [7–10].

However, quite a few excellent works have been presented so far to create an additional resonance in SIW CBSAs to obtain dual-band operation. Development of low profile SIW cavity-backed crossed slot antenna was reported in [11] for dual-frequency response. Dual-band characteristics can be consummated by using an L-shaped SIW slot antenna [12], a slot array antenna [13] with SIW

Received 12 February 2020, Accepted 27 March 2020, Scheduled 3 April 2020

* Corresponding author: Bollavathi Lokeshwar (lokesh5701@gmail.com).

¹ Department of ECE, Annamalai University, Annamalainagar, India. ² Department of IT, Annamalai University, Annamalainagar, India. ³ Department of ECE, R.V.R. & J.C College of Engineering, Guntur, India.

technology, a slot cut with dumbbell-shape design backed by SIW cavity [14], and a pair of stubs in the very center of a rectangular slot [15]. In [16], a ring slot having triangular shape is etched on a SIW cavity, where both the slot-mode and triangular-shaped patch within the slot (patch-mode) together are excited to attain two frequencies. In [17], a bow tie-shaped slot along with two special holes filled by a copper layer is embedded into the SIW cavity to generate dual-frequency response. A three-layer corrugated antenna with a low profile was reported in [18]. To accomplish a dual-band property in [18], cavity (resonant slot) and transmission line both impart one frequency individually. A dual-band cavity-backed antenna with two transverse slots based on SIW technique has been discussed in [19], in which two half modes of the cavity ensured the dual-frequency response.

In this work, the proposed design utilizes bilateral slots as radiating elements, which is a more distinctive feature than that of a cavity backed antennas with unilateral slots reported in [11–19]. These bilateral slots cause the quality factor of the SIW cavity to decrease, and as a result, two hybrid modes odd TE_{210} and half TE_{310} are excited to generate the two resonant frequencies operating in the X band and Ku band, respectively. One of the most desirable traits of the proposed design is frequency ratio (f_2/f_1), which can be tuned independently by changing the dimensions of the long and short slots or their positions individually. The fabricated prototype is then tested. It will be shown that the measured results are matching very well with the simulated ones.

2. ANTENNA CONFIGURATION

The formation of the proposed antenna goes through many stages as shown in Figure 1. SIW cavity is portrayed as stage I in Figure 1(a). Stage II is planned for single frequency design as shown in Figure 1(b). Similarly, stage III is for the dual-frequency antenna. A single dielectric substrate is utilized to configure the antenna completely for obtaining two frequencies. The schematic of the proposed dual-band antenna with bilateral slots is depicted in Figure 2. The SIW cavity of the proposed design is fully constructed on a same substrate, where the four sidewalls are implemented by four rows of metallic vias arranged uniformly along the edges of the antenna. Copper layer put to use the top and bottom walls of the cavity. To glean lower leakage losses between the successive vias and to make SIW cavity on a par to conventional metallic cavity, the cylinder diameter d and distance between the two adjacent vias (pitch) p are selected in such a way that they must satisfy the conditions of $p/d \leq 2$ and $d/\lambda_0 \leq 0.1$ [20].

A long transversal slot having length l_{s1} is placed on the ground plane from the upper sidewall of the SIW cavity with a short distance d_{su1} , and a short transversal slot of length l_{s2} is engraved at the

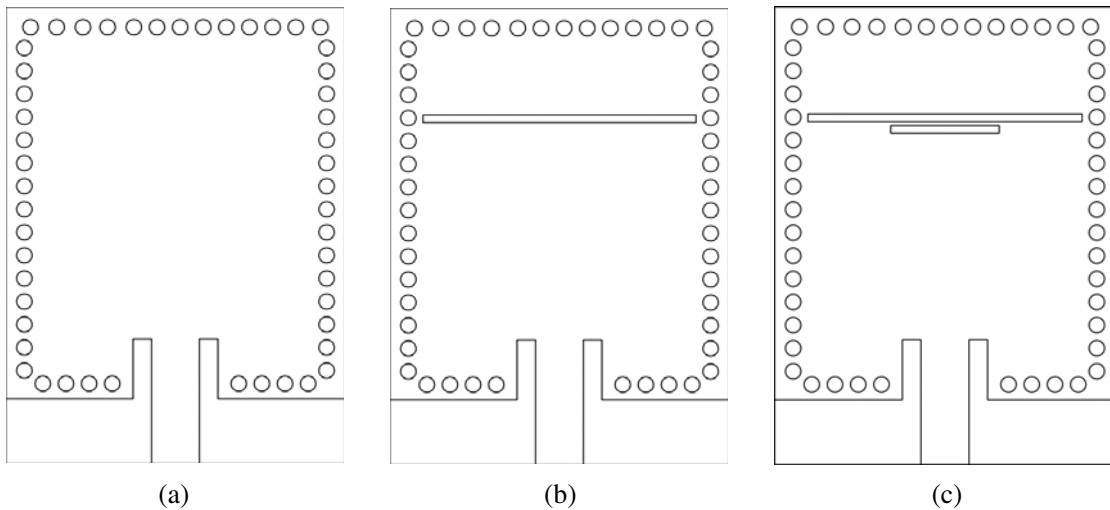


Figure 1. Development stages of the proposed dual-band SIW cavity backed antenna. (a) SIW cavity only (Stage I). (b) Single frequency antenna (with long transversal slot (Stage II)). (c) Dual frequency antenna (with bilateral slots (Stage III)).

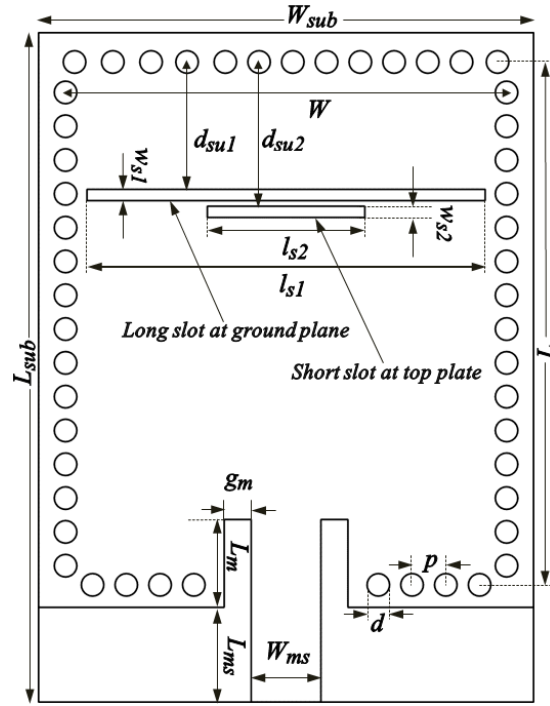


Figure 2. Geometry of the proposed dual-band antenna.

Table 1. Dimensional parameters of the proposed design (unit: mm).

Parameter	Value	Parameter	Value	Parameter	Value
W_{sub}	22	L_{ms}	4.2	L_{s2}	7
L_{sub}	29.7	L_m	3.9	d_{su1}	5.65
W	18.8	g_m	1.2	d_{su2}	6.4
L	23.2	$W_{s1} = W_{s2}$	0.5	p, d	1.5, 1
W_{ms}	3.1	L_{s1}	17.7	h	0.8

top of the cavity with a distance d_{su2} from the same sidewall of the cavity. It is worthwhile to note that there is an offset between the two slots to obtain dual-band frequency response. To facilitate the planar integration, a $50\ \Omega$ microstrip line followed by a $50\ \Omega$ grounded co-planar waveguide (GCPW) is used to excite the proposed antenna. The preliminary size of the SIW cavity which can be calculated by using the formula [21] of resonant frequency is given in Equation (1). Detailed geometrical parameters are tabulated in Table 1.

$$f_{mnp'} = \frac{1}{2\sqrt{\mu_0\epsilon_0\epsilon_r}} \sqrt{\left(\frac{m}{L_{eff}}\right)^2 + \left(\frac{n}{W_{eff}}\right)^2 + \left(\frac{p'}{h}\right)^2} \quad (1)$$

where m, n, p' are half-wave field variations in x, y and z -directions, respectively; ϵ_r is the dielectric constant of the substrate; equivalent length of the cavity (L_{eff}) = $L - \frac{d^2}{0.95 * p}$; equivalent width of the cavity (W_{eff}) = $W - \frac{d^2}{0.95 * p}$; d is the cylinder diameter; p is the distance between the two adjacent vias.

3. PRINCIPLE OF OPERATION

3.1. Antenna without Short Transversal Slot

In order to understand the loading effect of short slot, the SIW cavity antenna without slots (Stage I) and loaded with a long transversal slot (Stage II) of length above half wavelength is simulated using HFSS at first. Figure 3 represents the input resistance (Real Z_{11}) plot, where the generations of different hybrid modes are distinguished from the peaks of the input resistance curves. When the bilateral slots are not included in the SIW cavity (Stage I), TE_{110} , TE_{210} , and TE_{310} are generated at 7.15 GHz, 10.35 GHz, and 14.00 GHz, respectively. The electric filed distributions of these modes simulated from HFSS are shown in Figure 4. It is evident from input resistance (Real Z_{11}) plot that when a long transversal slot (Stage II) is introduced at the bottom metallic wall of the cavity, the conventional TE_{210} mode gets distorted slightly, and as a result, a new pair of hybrid modes is generated at 9.9 GHz and 10.4 GHz. These two hybrid modes are known as odd TE_{210} and even TE_{210} modes, since their electric fields indicate odd and even symmetries around the slot, respectively.

Similarly, TE_{310} mode of the unloaded cavity is perturbed, and the corresponding resonance gets shifted from 14 GHz to higher frequency, which consequently generates a non-resonant mode at 14.65 GHz. However, this TE_{310} mode is not involved in generating the resonant frequency in this case. Therefore, a long transversal slot in the single frequency design radiates at resonant frequency of 10 GHz. The mode obtained at this frequency is known as odd TE_{210} mode. Figures 5(a) and 5(b)

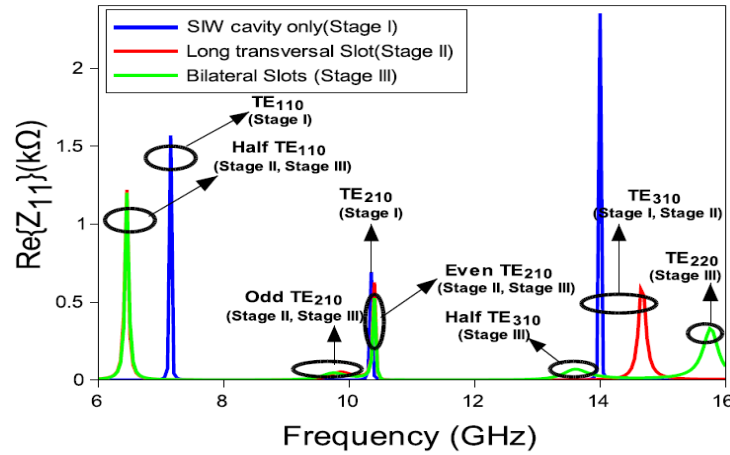


Figure 3. Input resistance (Real Z_{11}) curve of the SIW cavity only (Stage I), with long transversal slot (Stage II) and with bilateral slots (Stage III).

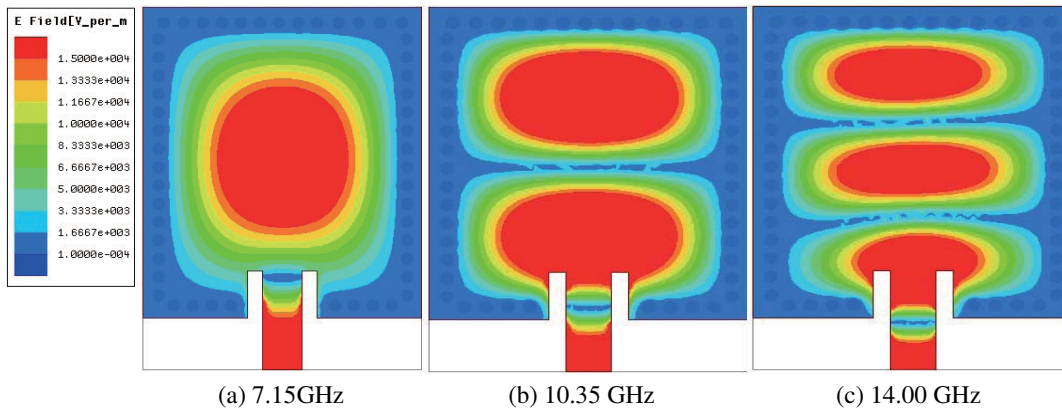


Figure 4. Electric field distributions of the cavity without bilateral slots (a) TE_{110} mode; (b) TE_{210} mode; (c) TE_{310} mode.

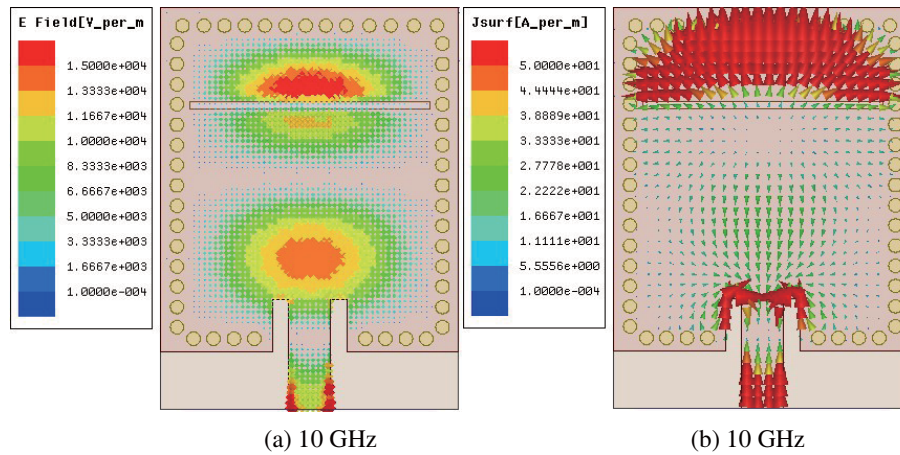


Figure 5. (a) Electric field vector and (b) surface current density vector simulated from HFSS for the single frequency design in odd TE_{210} mode.

represent the electric field and surface current distributions of the single frequency design at resonant frequency, respectively.

3.2. Antenna with Bilateral Slots

When the short transversal slot of length lower than the half-wave length is employed on the top metallic wall of the cavity, radiation of the antenna is generated at two distinct frequencies. The working principle of the proposed dual-frequency design (Stage III) is clearly understood by the simulated input resistance (Real Z_{11}) plot as shown in Figure 3. It is observed that the two hybrid modes odd TE_{210} and even TE_{210} remain almost unperturbed with the loading of a short slot, which suggests that this particular short slot has no effect on these two higher order modes. As a result, the lower resonant frequency (f_1) of the proposed design at odd TE_{210} mode is almost similar to the case of single frequency design. It is also seen that in this case, the conventional TE_{310} mode is distorted by sharing the electric field strength with long and short slots within the cavity, which results in generating a new set of hybrid modes in the cavity at 13.6 GHz and 15.75 GHz. Therefore, Stage III in Figure 3 reveals that TE_{310} mode gets perturbed when the short slot is incorporated in the cavity, and as a result, a higher resonant frequency (f_2) is obtained at half TE_{310} mode. It can also be identified that the generation of higher resonant mode has almost no effect on the lower resonant mode obtained at f_1 .

To elucidate the electromagnetic radiation properties of the proposed antenna with more intuition, electric field distribution of the antenna at two resonant frequencies is shown in Figure 6. It is evident that the electric field distributions of the dual-frequency design at lower resonant frequency ($f_1 = 9.8$ GHz) is almost similar to that of the odd TE_{210} mode of the single frequency design. Figure 6(a) depicts that at 9.8 GHz (odd TE_{210}), the electric field becomes dominant on the top side of the long transversal slot and minimum at the bottom side of the long slot. At this frequency, the magnitude of the electric field at two sides of the long slot is out of phase, which consequently helps the slot radiate electromagnetic waves into free space. It is also a fact that at 9.8 GHz, long slot plays a vital role behind the radiation.

However, the field distribution due to the short transversal slot is almost negligible at lower resonant mode, which indicates that lower resonant frequency (f_1) does not depend on the length of the short slot. Similarly, the higher resonant mode (f_2) is excited by the short slot at 13.8 GHz. Its electric field distribution plotted in Figure 5(b) shows that there is dominant electric field mostly located at either side of the short slot. By observing the electric field distribution, it is found that the electric field is situated in the overlap region of the long and short slots. Moreover, it is evident from Figure 5(b) that the incorporation of the long slot has almost no effect on the electric distribution at f_2 significantly. At this frequency, the electric field strength has opposite phases at two sides of the short slot, which can make the slot radiate into air.

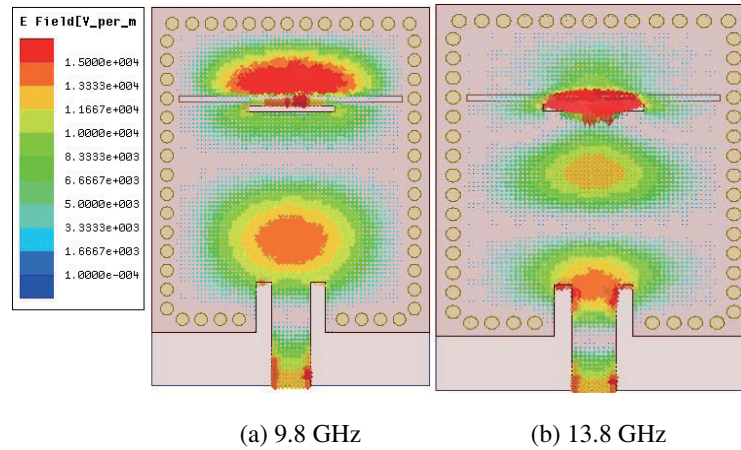


Figure 6. Electric field vector for the dual frequency design in (a) odd TE_{210} mode; (b) half TE_{310} mode.

3.3. Parametric Analysis

The effect of various critical parameters on the frequency response characteristic of the proposed design is explicated for further study by parametric analysis. This approach encourages the design of antennas for further practical use. The alterations of two resonant frequencies (f_1 , f_2) of the proposed antenna with the slot lengths (l_{s1} , l_{s2}), slot widths (w_{s1} , w_{s2}), and positions (d_{su1} , d_{su2}) are discussed in this section. It is noted that during parametric analysis, the value of parameter under inspection is only changed, and all the remaining optimized parameters are kept as listed in Table 1.

It is observed from Figures 7(a) and 7(b) that the operating frequencies f_1 and f_2 are in inverse proportion to the length of slots l_{s1} and l_{s2} , respectively. Figure 7(a) shows that as the length of the long slot l_{s1} increases from 16 mm to 18 mm, the lower operating frequency f_1 is reduced from 10.25 GHz to 9.65 GHz, while higher operating frequency f_2 remains constant at 13.8 GHz for a specific value of $l_{s2} = 7$ mm. Consequently, the frequency ratio (f_2/f_1) of the antenna in the range 1.34–1.43 can be achieved. In a similar way, the higher resonant frequency f_2 is shifted downward from 13.8 GHz to 12.2 GHz by increasing l_{s2} from 7 mm to 8 mm at step of 0.5 mm as illustrated in Figure 7(b). Simultaneously, the lower resonant frequency f_1 is almost invariable, and the frequency ratio (f_2/f_1) of the proposed design is obtained within the limits of 1.24 to 1.42.

The effect of slot widths w_{s1} and w_{s2} on impedance matching is plotted in Figures 8(a) and 8(b), respectively. It is identified from Figure 8(a) that when long slot width w_{s1} is changed, the lower and

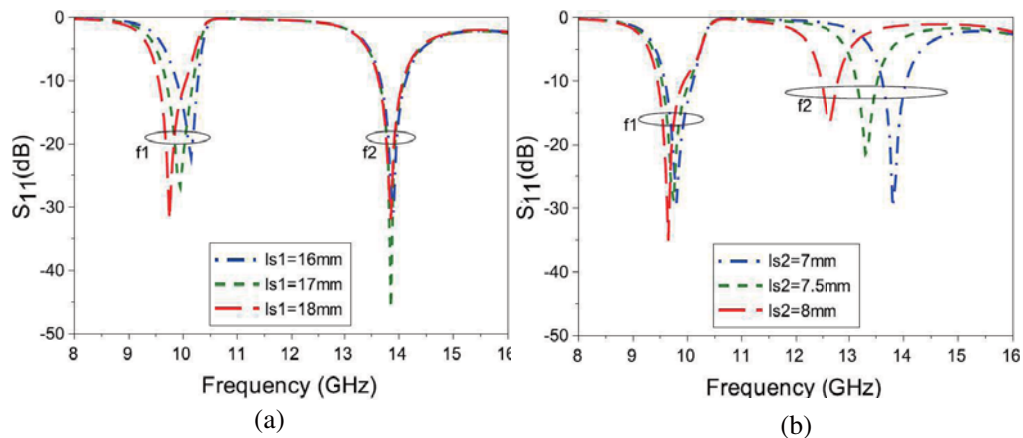


Figure 7. Reflection coefficient variation (S_{11}) by changing slot length (a) l_{s1} , (b) l_{s2} .

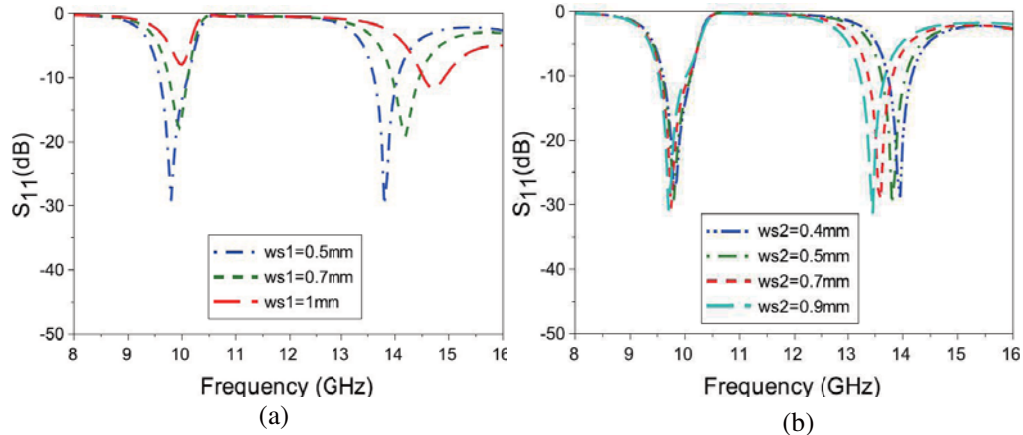


Figure 8. Reflection coefficient variation (S_{11}) by changing slot width (a) w_{s1} , (b) w_{s2} .

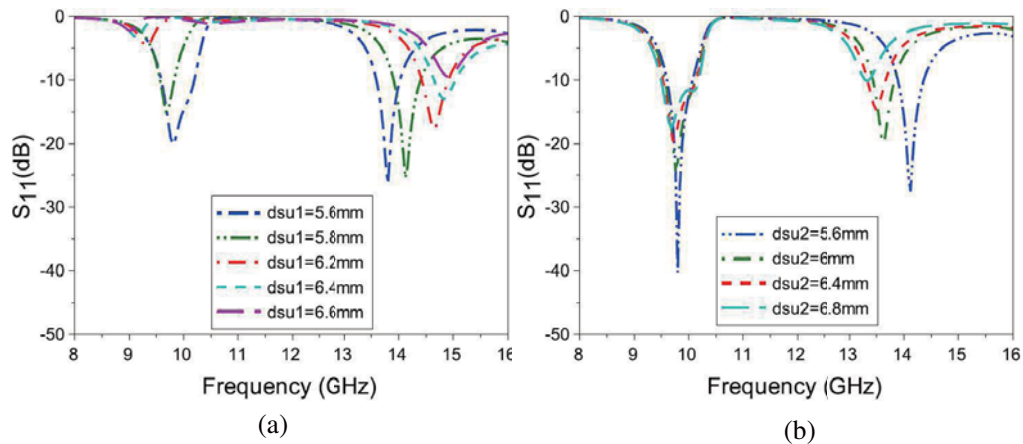


Figure 9. Reflection coefficient variation (S_{11}) by changing slot position (a) d_{su1} , (b) d_{su2} .

upper resonant frequencies can be moved to higher values, and impedance matching is greatly affected. As shown in Figure 8(b), width w_{s2} of short slot has no effect on the lower resonant frequency. However, upper resonant frequency can be changed within the limits of 14.1 GHz to 13.35 GHz by changing the w_{s2} value from 0.4 mm to 0.9 mm, and the impedance matching is almost unchanged when w_{s2} gets increased. Thereby, the frequency ratio (f_2/f_1) can be tuned from 1.36 to 1.44.

The influences of the long slot d_{su1} and short slot d_{su2} positions from upper side wall of the cavity have been analyzed individually in Figures 9(a) and (b), respectively. It can be clearly said that by shifting the positions of either d_{su1} or d_{su2} , the offset between the long slot and short slot can be changed. As shown in Figure 9(a), the variation in the value of d_{su1} from 5.6 mm to 6.6 mm in step size of 0.2 mm leads to disturbance in the current path, and as a result, the return loss of the antenna at both resonant frequencies is considerably reduced. In contrast, as plotted in Figure 9(b), when d_{su2} increases there is no change in the 9.8 GHz frequency. Concurrently, the 13.8 GHz resonant frequency is moved to lower values. Accordingly, the frequency ratio (f_2/f_1) can be attained around 1.31 to 1.52. Finally, it is concluded from the parametric analysis that by individually switching the parameters l_{s1} , l_{s2} , w_{s2} , d_{su2} of the proposed antenna along optimized values, both f_1 and f_2 can be tuned in itself. Thus, this parametric study puts forward the design to have more flexibility for the antenna designer.

4. RESULTS AND DISCUSSION

To corroborate the simulated prediction of the proposed design, a specimen of the antenna was manufactured with “printed circuit board” technology. Copper cladding substrate named RT/duroid5880 having a 0.8 mm standard thickness and dielectric constant 2.2 is employed in the

fabricated prototype. The perspective view of the proposed antenna is shown in Figure 10(a), and photographs of the fabricated prototype with top, bottom, and side views are shown in Figures 10(b), 10(c), and 10(d), respectively. The fabricated prototype is tested, and its reflection coefficient (S_{11}) is measured with the aid of vector network analyzer. The simulated and experimental results of the reflection coefficient (S_{11}) confirm the dual-band response as depicted in Figure 11. The simulation results of the single-frequency design are also included in Figure 11 to study the dual-band response. The simulated reflection coefficient manifests dual-band response at 9.8 GHz and 13.8 GHz, respectively. It can be substantiated from Figure 11 that the measured lower and upper resonant frequencies 9.85 GHz and 14 GHz, respectively, are almost close to simulated results. The gain performance of the antenna in the range 9.5 to 10.5 GHz and 13.5 to 14.5 GHz is also illustrated in Figure 11.

The simulated and measured impedance bandwidths (for below -10 dB) are 520 MHz and 530 MHz at lower operating frequency, respectively. Similarly, the simulated and measured impedance bandwidths (for below -10 dB) are 450 MHz and 440 MHz at the upper operating frequency, respectively. Thus, the measured reflection coefficient results show excellent semblance with the simulated results with a slight deviation. The simulated gain remains consistent and achieves peak gains of 6.78 dBi and 6.75 dBi at

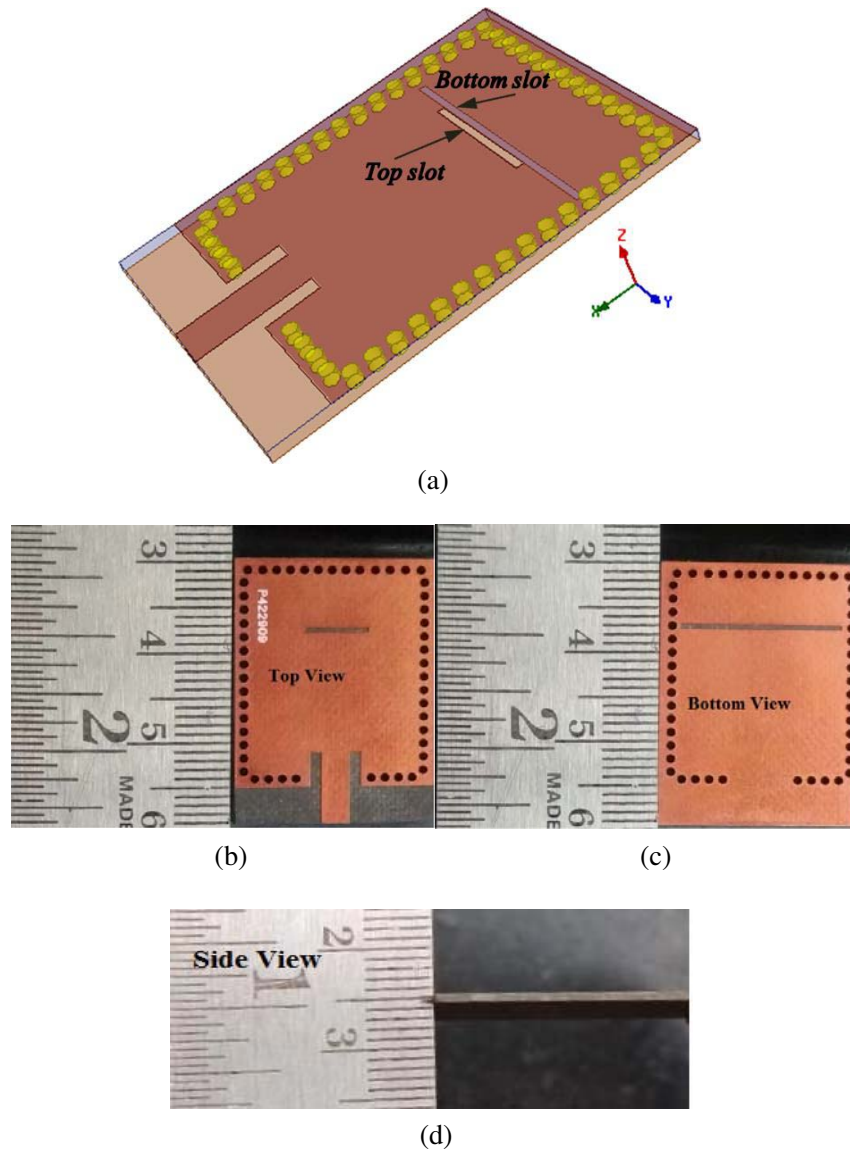


Figure 10. (a) Perspective view of the proposed antenna and (b) top view, (c) bottom view, (d) side view of the fabricated prototype.

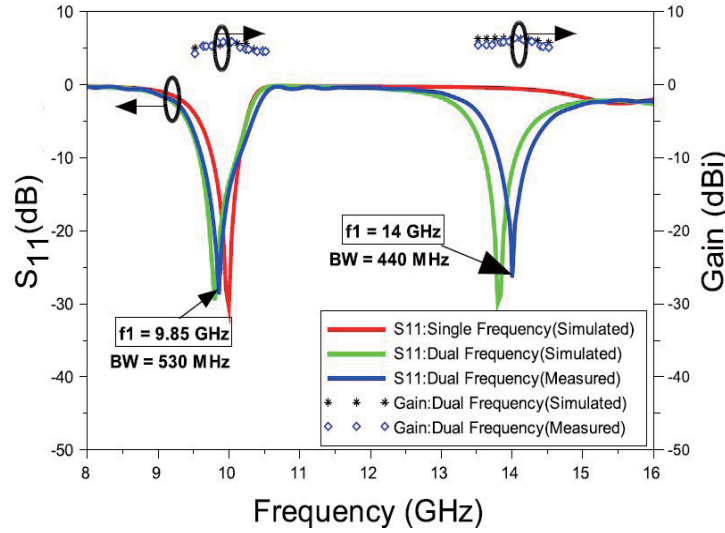


Figure 11. Comparison between simulated and measured results of reflection coefficient (S_{11}) and gain of the proposed antenna.

Table 2. Comparison among proposed antenna and some previously reported SIW CBSA.

Properties		Proposed work	[11]	[12]	[13]	[14]	[15]	[16]	[18]
Resonant frequency (GHz)	f_1	9.85	9.5	10.93	8.68	9.4	8.96	9.4	10
	f_2	14	10.5	12.69	10.8	13.62	15.84	16.2	12.18
Operating frequency band	f_1	X	X	X	X	X	X	X	X
	f_2	Ku	X	Ku	X	Ku	Ku	Ku	Ku
FBW (%)	f_1	5.48	1.8	1.55	0.92	2.02	2.67	1.4	2.7
	f_2	3.15	2.1	1.41	1.57	1.46	1.89	5.9	1.9
Gain (dBi)	f_1	6.62	5.5	6.58	7.71	5.3	4.47	4.86	12.5
	f_2	6.44	5.5	6.82	9.08	4.3	5.4	6.15	11.3
Frequency Ratio (f_2/f_1)		1.24 to 1.52	1.1–1.48	NM	NM	1.3–1.55	1.76	1.16–1.74	NM
Substrate thickness (mm)		0.8	0.5	NM	0.787	0.787	0.787	1.57	3.175
Permittivity		2.2	2.2	NM	2.2	2.2	2.2	2.2	4.5
Front-to-Back-Ratio (dB)		18.6	20.8	NM	NM	14	12	18	NM

f_1 — lower resonant frequency; f_2 — higher resonant frequency; NM — not mentioned

9.8 GHz and 13.8 GHz, respectively. The measured peak gains of 6.62 dBi at 9.85 GHz and 6.44 dBi at 14 GHz have been achieved, which are almost close to the simulated counterpart.

Figure 12 illustrates the simulated normalized far-field pattern of the dual-band antenna in two cut-planes, which are corresponding to XZ -plane ($\phi = 0^\circ$) and YZ -plane ($\phi = 90^\circ$) at lower and upper frequencies. The measured antenna pattern in the aforementioned two cut-planes is also included in the figure for comparison. As a consequence of bilateral slots engraved on a SIW cavity, the proposed antenna achieves unidirectional pattern at 9.85 GHz and bidirectional pattern at higher frequency 14 GHz. It is found from the measured results that the peak cross-polarization values in either plane are lower than -25 dB at a lower resonant frequency in the broadside direction. At 14 GHz, the peak cross-polarization levels are -20 dB, -17 dB in the XZ -plane and YZ -plane, respectively. However, a little inconsistency is found in measured radiation patterns against simulated radiation pattern, which can be attributed to fabrication imperfection. The half-power beamwidths of the co-polarized radiation pattern in XZ -plane and YZ -plane are about 111° and 75° , respectively, in the lower band. Similarly, they are 60° and 50° at XZ plane and YZ plane, respectively, in the upper band.

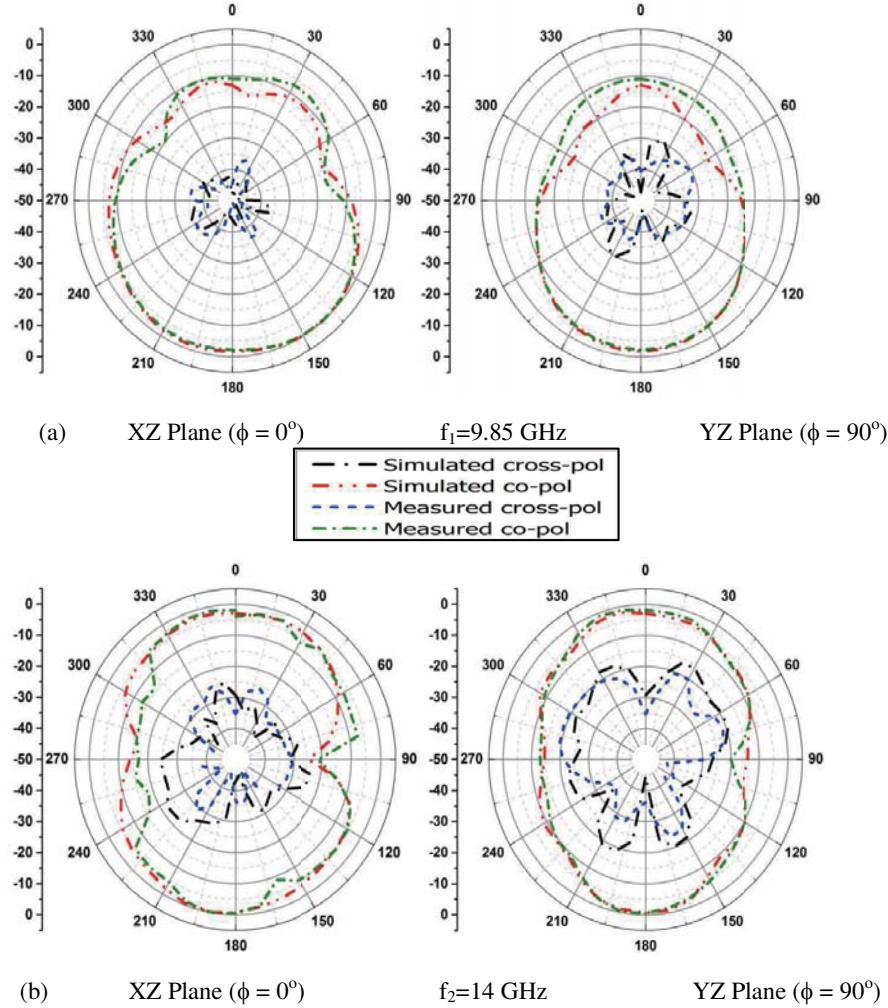


Figure 12. Simulated and measured normalized radiation patterns in XZ -plane and YZ -plane of the proposed dual-band antenna at (a) 9.85 GHz, (b) 14 GHz.

To highlight the essence of the proposed work, the comparative study between the proposed antenna and previously reported antennas is tabulated in Table 2. It may be observed that the proposed structure showcases the versatility in tuning the frequency ratio independently. It also renders a better bandwidth performance and possesses good gain at two frequencies as compared to works presented in [11–16, 18] by using bilateral slots.

5. CONCLUSION

A profound study of a dual-band cavity backing antenna with bilateral slots using SIW technology is discussed. In this design, horizontal slots etched at top and bottom of the cavity near the upper sidewall of the cavity has been used to perturb the conventional modes of the cavity. As a result, odd TE_{210} mode and half TE_{310} modes are generated, which create two resonant frequencies. In addition, independent tuning in the frequency ratio has been achieved by changing the slot dimensions and slot positions. Experimental results confirm that the proposed design creates dual-band response at 9.85 GHz with fractional bandwidth of 5.48% and at 14 GHz with fractional bandwidth of 3.15%. The antenna shows good enough performance with a stable gain of more than 5.4 dBi in the two operating bands and exhibits low cross polarization level at both the frequencies. Finally, with improved bandwidth at both the frequencies and enough gain, the proposed antenna is a suitable candidate for X/Ku band applications.

REFERENCES

1. Yoshimura, Y., "A microstrip slot antenna," *IEEE Trans. Microw. Theory Tech.*, Vol. 20, No. 11, 760–762, Nov. 1972.
2. Chem, J. S., "Dual-frequency annular-ring slot antennas fed by CPW feed and microstrip line feed," *IEEE Trans. Antennas Propag.*, Vol. 53, No. 1, 569–571, Jan. 2005.
3. Omar, A. A., M. C. Scardelleti, Z. M. Hejazi, and N. Dib, "Design and measurement of self-matched dual-frequency coplanar waveguide-fed-slot antennas," *IEEE Trans. Antennas Propag.*, Vol. 55, No. 1, 569–571, Jan. 2007.
4. Chen, Z. and Z. Shen, "A conformal cavity-backed supergain slot antenna," *IEEE Antennas Propag. Society Int. Symposium (APSURSI)*, 1288–1289, Sep. 2014.
5. Deslandes, D., and K. Wu, "Integrated microstrip and rectangular waveguide in planar form," *IEEE Microwave Wireless Compon. Lett.*, Vol. 11, No. 2, 68–70, Feb. 2001.
6. Bozzi, M., A. Geordiadis, and K. Wu, "Review of substrate-integrated waveguide circuits and antennas," *IET Microw. Antennas Propag.*, Vol. 5, No. 8, 909–920, 2011.
7. Luo, G. Q., Z. F. Hu, L. X. Dong, and L. L. Sun, "Planar slot antenna backed by substrate integrated waveguide cavity," *IEEE Antennas Wireless Propag. Lett.*, Vol. 7, No. 8, 236–239, Aug. 2008.
8. Bohorquez, J. C., H. A. F. Pedraza, et al., "Planar substrate integrated waveguide cavity-backed antenna," *IEEE Antennas Wireless Propag. Lett.*, Vol. 8, 1139–1142, 2009.
9. Lacik, J., T. Mikulasek, Z. Raida, and T. Urbanec, "Substrate integrated waveguide monopolar ring-slot antenna," *Microwave & Optical Technology Letters*, Vol. 56, No. 8, 1865–1869, Aug. 2014.
10. Mukherjee, S., A. Biswas, and K. V. Srivastava, "Bandwidth enhancement of substrate integrated waveguide cavity backed slot antenna by offset feeding technique," *IEEE Applied Electromagnetics. Conf. (AEMC)*, Dec. 2013.
11. Luo, G. Q., Z. F. Hu, Y. Liang, et al., "Development of low profile cavity backed crossed slot antennas for planar integration," *IEEE Trans. Antennas Propag.*, Vol. 57, No. 10, 2972–2979, Oct. 2009.
12. Srivastava, A., R. K. Chaudhary, A. Biswas, and M. J. Akhtar, "Dual-band L-shaped SIW slot antenna," *Int. Conference on Microwave and Photonics (ICMAP)*, 2013.
13. Mukherjee, S., K. V. Srivastava, and A. Biswas, "Implementation of dual-frequency longitudinal slot array antenna on substrate integrated waveguide at X-band," *Proc. of Eur. Microw. Conf. (EuMC)*, 195–198, Oct. 2013.
14. Mukherjee, S., A. Biswas, and K. V. Srivastava, "Substrate integrated waveguide cavity backed dumbbell-shaped slot antenna for dual frequency operation," *IEEE Antennas Wireless Propag. Lett.*, Vol. 14, 1314–1317, 2015.
15. Mukherjee, S., A. Biswas, and K. V. Srivastava, "Substrate integrated waveguide cavity backed slot antenna for dual-frequency application," *IEEE Eur. Microw. Conf. (EuMC)*, 57–60, Oct. 2014.
16. Zhang, T., W. Hong, Y. Zhang, and K. Wu, "Design and analysis of SIW cavity backed dual-band antennas with a dual-mode triangular ring slot," *IEEE Trans. Antennas Propag.*, Vol. 62, No. 10, 5007–5016, Oct. 2014.
17. Nandi, S. and A. Mohan, "Bowtie slotted dual-band SIW antenna," *Microwave & Optical Technology Letters*, Vol. 58, No. 10, 2303–2308, Oct. 2016.
18. Honari, M. M., R. Mirzavand, H. Saghlatoon, and P. Mousavi, "A dual-band low profile aperture antenna with substrate integrated waveguide grooves," *IEEE Trans. Antennas Propag.*, Vol. 64, No. 4, 1561–1566, Apr. 2016.
19. Niu, B. J., J. H. Tan, and C. L. He, "SIW cavity-backed dual-band antenna with good stopband characteristics," *IET Electron. Lett.*, Vol. 54, No. 22, 1259–1260, 2018.
20. Xu, F. and K. Wu, "Guided-wave and leakage characteristics of substrate integrated waveguide," *IEEE Trans. Microw. Theory Tech.*, Vol. 53, No. 1, 66–73, Jan. 2005.
21. Wu, Q., J. Yin, et al., "Broadband planar SIW cavity-backed slot antennas aided by unbalanced shorting vias," *IEEE Antennas Wireless Propag. Lett.*, Vol. 18, No. 2, 363–367, 2019.